Rev. Roum. Sci. Techn.– Électrotechn. et Énerg.
Vol. **64**, *1*, pp. 75–80, Bucarest, 2019

Automatique et ordinateurs

GAIN-SCHEDULED PROPORTIONAL INTEGRAL DERIVATIVE CONTROL OF TAXI MODEL OF UNMANNED AERIAL VEHICLES

MARYAM WASIM[1], MUKHTAR ULLAH[1], JAMSHED IQBAL[1,2]

Key words: Taxi phase, Unmanned aerial vehicle (UAV), Proportional integral derivative (PID), Gain scheduled (GS).

Unmanned aerial vehicles (UAVs) are extensively used for defense and surveillance applications. To ensure desirable performance under all conditions, a UAV requires an appropriate control strategy. For the design of control law, a complete understanding of the model is necessary. The present research proposes and develops a control strategy for a three-wheeled UAV while it is in taxi phase. This necessitates conducting a control-oriented analysis on the UAV to determine the most efficient input channel for controlling a specific output. A control structure is then designed to control the outputs using the control input of nose-wheel steering angle and rudder. In this regard, a proportional integral derivative (PID) controller offers a preliminary solution. To cater for the highly nonlinear nature of the taxi model, we propose a solution that employs a gain-scheduled PID (GS-PID) controller to cover the entire operating range of the UAV during taxi phase, where speed of the UAV is a scheduling variable. The values of the controller parameters are continuously updated according to the current UAV speed. Simulation results in the form of trajectory tracking in the presence of disturbances demonstrate efficiency of the proposed control law.

1. INTRODUCTION

Control systems are an integral part of industrial applications for example automation, transportation, manufacturing, home appliances and many more [1]. To ensure proper working of any system, its control is necessary [2]. Proper implementation of any control strategy requires control system design and for that deep analysis of the model is required [3]. This work presents analysis and control of taxi model of three-wheeled unmanned aerial vehicle (UAV) designed for a defense application. Before starting with controller design and implementation, it is necessary to understand the behavior and dynamics of a UAV while it is in taxi phase. Control oriented analysis of the UAV can highlight the different channels through which the outputs of the UAV can be controlled.

The taxi model of an UAV is inherently non-linear and gain scheduling has been selected to control it. Gain scheduling involves selecting a reference trajectory and then using this reference trajectory for selecting some operating points. At each of these points, the system is linearized and a separate controller is designed for each operating point. Various control techniques have been covered in literature for UAV with both longitudinal and lateral control. However, the focus of this research is control structure design for ground motion of a three-wheeled UAV.

The classic PID controller, or the three-term controller, has been reported in [4] and lateral control of UAV taxiing phase is done using a combination of rudder and nose wheel steering. In [5], after developing the model, a lateral controller is designed, which is simply a proportional gain to control the heading angle. After developing a taxi model for UAV, the control scheme reported in [6] is then developed for automatic takeoff. The longitudinal control law and runway steering control are separately developed. The simulation results prove that the controller developed is very accurate and the control law is also efficient.

In [7], the focus is to develop an automatic takeoff system which is based on active disturbance rejection control (ADRC) so that the UAV can take off safely even when the wind conditions are not normal. The results show that the UAV experiences safe takeoff when the downburst is less than 13 m/s. In [8], various control strategies are tested on a fixed-wing UAV during taxiing phase. The linearized and decoupled lateral model is controlled by applying adaptive internal model control (AIMC). Different control strategies are tested and compared and finally the control strategy with rudder and nose wheel steering angle has been selected as the most efficient.

Automatic tuning of attitude control system for a UAV has been discussed in [9]. It can be applied to unstable or critically stable open loop poles. A cascade proportional integral (PI) control structure is configured in a closed loop control fashion. This work has been extended in [10] by implementing gain scheduled PID control system for a fixed wing UAV. This is done by designing a family of proportional integral derivative (PID) cascade control systems for certain operating conditions of airspeed.

A sliding mode control (SMC) strategy is used in [11] for the control of fixed-wing UAV in the presence of wind perturbation. The controller design is based on a full nonlinear mathematical model which includes the stochastic wind effects. An extended Kalman filter (EKF) is used for filtering and state estimation. In [12] another method of high level nonlinear model predictive control (MPC) is reported. The controller is designed for lateral-directional UAV trajectory tracking in wind.

A lateral guidance scheme based on nonlinear sliding surface has been proposed in [13] for UAVs with limited actuation control. The objective of the lateral guidance scheme is to make the cross track error zero. This scheme follows the inner and outer loop structure for control and guidance respectively. Artificial intelligence has been used in [14] for automatic flight control. The designed controllers are based on the theory of linear quadratic regulators (LQR). The feedback gain is obtained for every flight condition and is then fed to the system. Another neural controller has been proposed in [15] to replace the

[1] Department of Electrical Engineering, National University of Computer and Emerging Sciences, Islamabad, Pakistan, mukhtar.ullah@nu.edu.pk
[2] Department of Electrical and Electronics Engineering, University of Jeddah, Saudi Arabia.

classical digital controller of an airborne warning and control system (AWACS) aircraft. In this case the simulations which had the objective to track a missile target showed that the proposed neural controller exhibits better performance than a classical one. Moreover, an added advantage is that the neural controller is cheaper and lighter than a classical controller.

This work presents a technique of GS-PID control for a nonlinear taxi model of a three-wheeled UAV. Control-oriented analysis is performed before designing a control structure for the UAV. Simulations include testing the proposed technique under disturbances such as wind. This paper is organized as follows: Section 2 presents the system model, Section 3 discusses the control-oriented analysis of the UAV taxi model. Section 4 gives the technique used for the control of UAV and Section 5 presents the results that highlight the performance of the proposed control technique used. Finally, in Section 6 there are the comments and conclusions.

2. SYSTEM MODEL

Owing to the fact that UAV model is inherently non-linear, it is necessary to perform detailed analysis of the model. The UAV under consideration has a mass of 550 kg. There are 4 inputs to the UAV: rudder, nose wheel steering, left brake and right brake. The limitations of each input are: rudder limit (–3, 3) deg, steering angle limit (–1, 1) deg and brakes limit (0, 60) %.

Since the focus of the present work is on the taxi model of UAV, the corresponding desired outputs are mentioned in Table 1. Y position y in earth fixed (EFX) frame indicates the deviation of UAV from the center line of the runway. Yaw angle ψ is the deviation from the center line in X-Y body (BDY) frame. Body rate r is the derivative of the yaw angle, also known as yaw rate.

Table 1
Output from UAV

Desired outputs from UAV	Unit	Symbol
Y position in EFX-frame	m	y
Body rate in BDY-frame	deg/s	r
Yaw angle	deg	ψ

The equations of motion of a UAV on ground for a non-rotational flat earth model can be written as shown in equations (1)-(5).

$$\dot{\bar{p}} = B^T (\bar{v} + \bar{w} + \overline{r_{cg}}) \tag{1}$$

$$\dot{\bar{v}} = -\bar{\omega}\times\bar{v} - \dot{\bar{\omega}}\times\overline{r_{cg}} - \bar{\omega}\times\left(\bar{\omega}\times\overline{r_{cg}}\right) + \bar{F}/m \tag{2}$$

$$\dot{\bar{\omega}} = -J^{-1}\left[\bar{\omega}\times\left(J\bar{\omega}\right)\right] + J^{-1}\bar{M} \tag{3}$$

$$\bar{\theta} = f\left(\bar{\theta}\right)\bar{\omega} \tag{4}$$

$$\dot{\omega}_i = \frac{M_i}{J_i}, i \in \{f, rl, rr\}, \tag{5}$$

where

- $\bar{p} = [x, y, z]^{\mathrm{T}}$ is the center of gravity (COG) position in EFX frame.
- B is the transformation matrix from EFX to BDY.
- $\bar{v} = \left[v_x, v_y, v_z\right]^{\mathrm{T}}$ is the linear velocity of the center of rear axle expressed in BDY frame.
- $\bar{\omega} = \left[\omega_x, \omega_y, \omega_z\right]^{\mathrm{T}}$ is the angular velocity of the body frame with respect to inertial earth fixed frame expressed in body frame.
- $\overline{r_{cg}} = \left[c, 0, -h_{cg} + R_r\right]^{\mathrm{T}}$ is the position vector from center of rear axle to center of gravity (cg) and h_{cg} is the height of COG from ground.
- $\bar{F} = \left[F_x, F_y, F_z\right]^{\mathrm{T}}$ and $\bar{M} = \left[M_x, M_y, M_z\right]^{\mathrm{T}}$ are respectively the total force and moment expressed in body frame.
- $\bar{\theta} = [\phi, \theta, \psi]^{\mathrm{T}}$ are the Euler's angles of the BDY fixed frame with respect to E frame.
- $\left[\omega_f, \omega_{rl}, \omega_{rr}\right]^{\mathrm{T}}$ are the wheel's angular velocity. The subscript f is for the front wheel, rr is for the rear right and rl is for the rear left wheel.
- The inertia matrix J and the matrix $f\left(\bar{\theta}\right)$ are given by,

$$J = \begin{bmatrix} J_x & 0 & -J_{xz} \\ 0 & J_y & 0 \\ -J & 0 & J_z \end{bmatrix}, \tag{6}$$

$$f\left(\bar{\theta}\right) = \begin{bmatrix} 1 & \tan\theta\sin\phi & \tan\theta\cos\phi \\ 0 & \cos\phi & -\sin\phi \\ 0 & \dfrac{\sin\phi}{\cos\theta} & \dfrac{\cos\phi}{\cos\theta} \end{bmatrix}. \tag{7}$$

3. CONTROL-ORIENTED ANALYSIS OF UAV

The control inputs of UAV have different effects on the UAV behavior. To ensure that an appropriate input is being used for the control of UAV, we have to first determine the input channels which are more effective in controlling the outputs of UAV. The effect of rudder input and nose wheel steering input is analyzed by applying a step signal at 1 s, which taking into account the effect on all three outputs y, r and ψ. Figures 1 and 2 show the results of this analysis. When no input is applied to the UAV, the outputs do not change, so the UAV stays on the centerline and does not steer away from it. However, if the UAV is applied with both inputs, rudder and steering wheel, it starts to steer away from the centerline. This shows that these inputs have an effect on the outputs of UAV and therefore, can be used to control the UAV. If the UAV is moving away from the centerline during taxi phase due to some disturbances, these inputs can be used to bring the UAV back to the centerline.

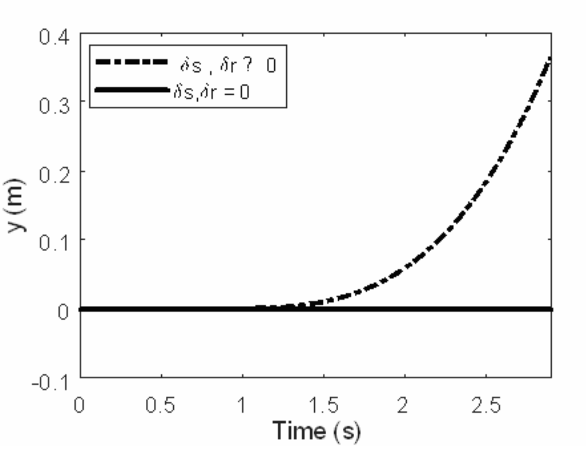

Fig. 1–Effect on y by applying inputs

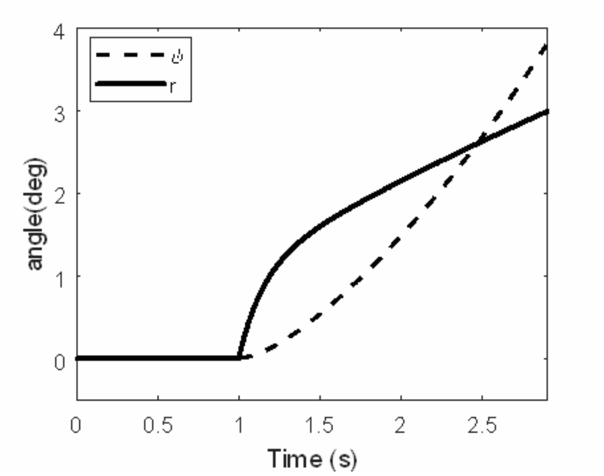

Fig. 2–Effect on r and ψ by applying inputs, both are zero without input.

4. GAIN SCHEDULED PID CONTROL OF UAV

The GS-PID control has been implemented in both MATLAB R2017a and Simulink. The sequence followed for the control of UAV is depicted in the flow chart given in Fig. 3.

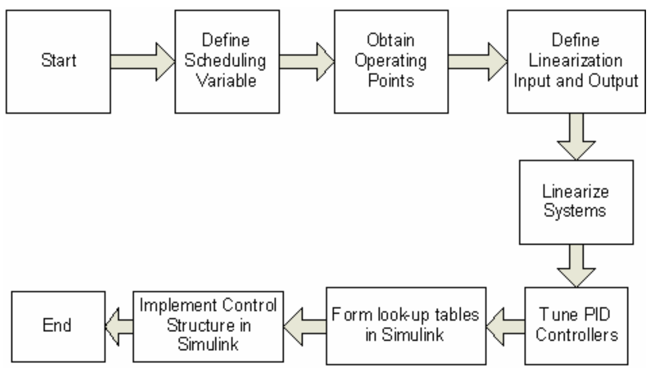

Fig. 3– Flow chart for implementation of GS-PID controller.

The velocity of UAV $u = v_x$ as shown in Fig. 5 has been selected as a scheduling variable for the UAV. It covers the whole operating range of the taxi model of UAV. The inputs used for the control of UAV taxi model and to regulate the outputs include nose wheel steering angle δ_s and rudder input δ_r. The open loop model of the UAV was linearized around a specific operating trajectory by selection of open loop input and open loop output. The MATLAB command used for the linearization of UAV is ‘linearize’. In this step, the bode plot of the linearized model is also obtained using ‘bode’. Figure 4 shows the overall control structure for the UAV and Fig. 5 gives a detailed insight in the GS-PID controllers. The command ‘pidtune’ is used in MATLAB to tune theses controllers to achieve best possible result. After tuning, the gains are saved in ‘lookup table’ using Simulink where each PID controller is provided with gains according to the value of the scheduling variable u which is the velocity of the UAV. The UAV taxi phase controller shown in Fig. 4 can be analytically formulated by Equations (8)-(9), where y_ref, r_ref and ψ_ref are the reference signals. y, r and ψ are the outputs from the UAV taxi model. GS-PID controllers are actually two controllers. Note that in Equations (8) and (9) the subscripts in each gain K indicates the type of controller, proportional (P), integral (I) and derivative (D) and the superscript indicates the input output combination.

$$\begin{aligned}\delta_s = &\left(K_P^{y\delta s} + K_I^{y\delta s} + K_D^{y\delta s}\right) * \left(y - y\_ref\right) + \\ &\left(K_P^{r\delta s} + K_I^{r\delta s} + K_D^{r\delta s}\right) * \left(r - r\_ref\right) + \\ &\left(K_P^{\psi\delta s} + K_I^{\psi\delta s} + K_D^{\psi\delta s}\right) * \left(\psi - \psi\_ref\right)\end{aligned} \tag{8}$$

$$\begin{aligned}\delta_r = &\left(K_P^{y\delta r} + K_I^{y\delta r} + K_D^{y\delta r}\right) * \left(y - y\_ref\right) + \\ &\left(K_P^{r\delta r} + K_I^{r\delta r} + K_D^{r\delta r}\right) * \left(r - r\_ref\right) + \\ &\left(K_P^{\psi\delta r} + K_I^{\psi\delta r} + K_D^{\psi\delta r}\right) * \left(\psi - \psi\_ref\right)\end{aligned} \tag{9}$$

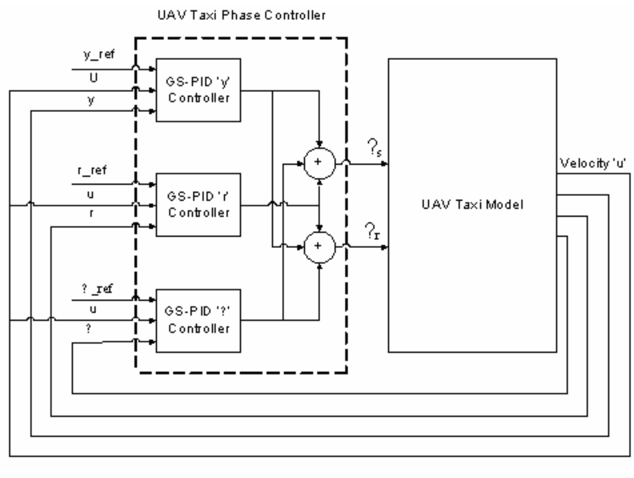

Fig. 4–Control structure for taxi model of UAV.

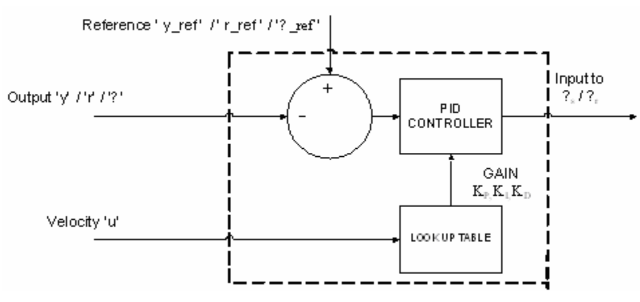

Fig. 5–GS-PID controller.

5. **SIMULATION**

The designed control law for UAV is tested and analyzed in MATLAB (R2017a) and Simulink running on 64 bit Windows 7 operating system installed on a 2.5 GHz core i-5 CPU and with a RAM of 6 GB. The UAV is initially tested under normal conditions and then with a disturbance of wind with a magnitude 2 m/s and 6 m/s.

5.1. VALUES OF SCHEDULING VARIABLE

Gain scheduling requires the controller gains to be continuously updated and this task is carried out with the help of a scheduling variable u in this case. Four different points from Fig. 6 are used as operating points between t = 0 s to t = 3 s. Figure 6 shows the graph of scheduling variable with time. The linear velocity of UAV is increasing as it speeds down the runway.

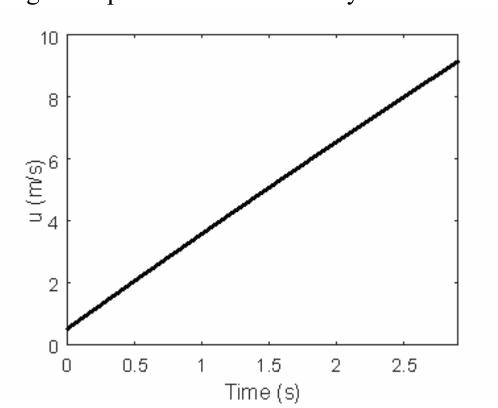

Fig. 6–Scheduling variable u *vs.* time.

5.2. LINEARIZATION OF TAXI MODEL

The UAV is linearized at various combinations of input and output corresponding to four different operating points since there are three outputs and two inputs used for the linearization of UAV. Figures 7 – 12 present bode plot for various combinations showing the magnitudes at first four operating points. As can be seen, the system dynamics vary at each operating point. Therefore, the same PID gains cannot be used over the whole operating range of the UAV. It is also pertinent to notice that at each input output combination, the linearized model of the system has a different behavior.

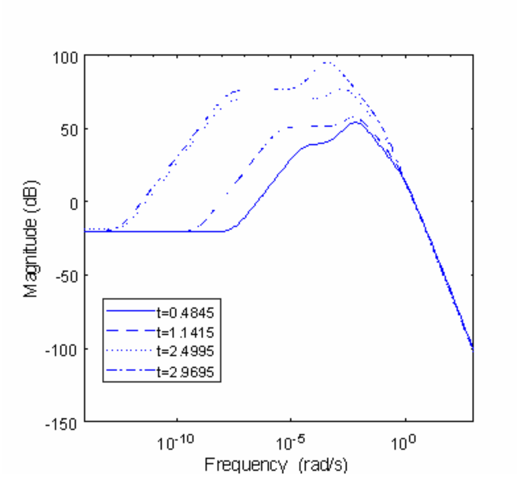

Fig. 7–Bode plot of δ_s to ψ

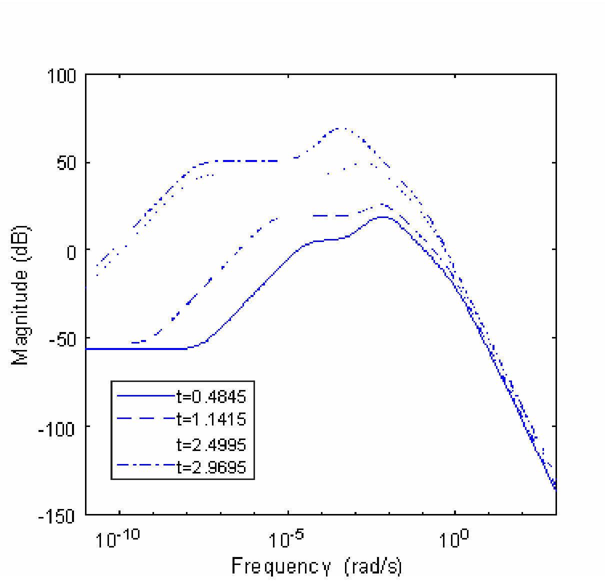

Fig. 8–Bode plot of δ_r to ψ

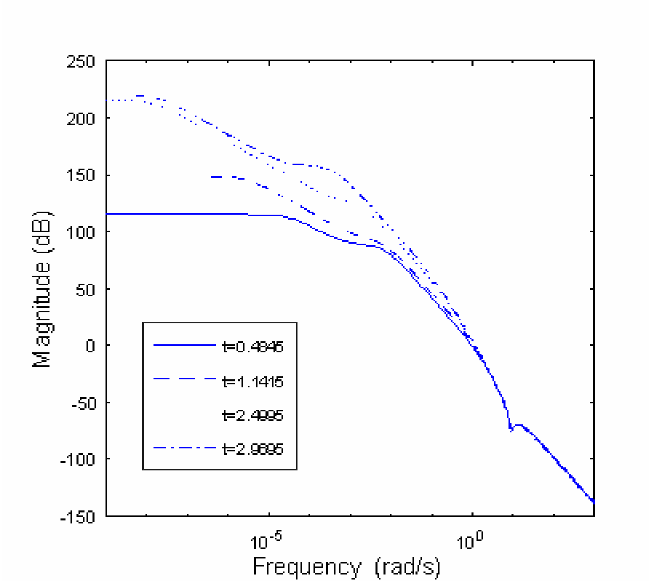

Fig. 9–Bode plot of δ_s to y

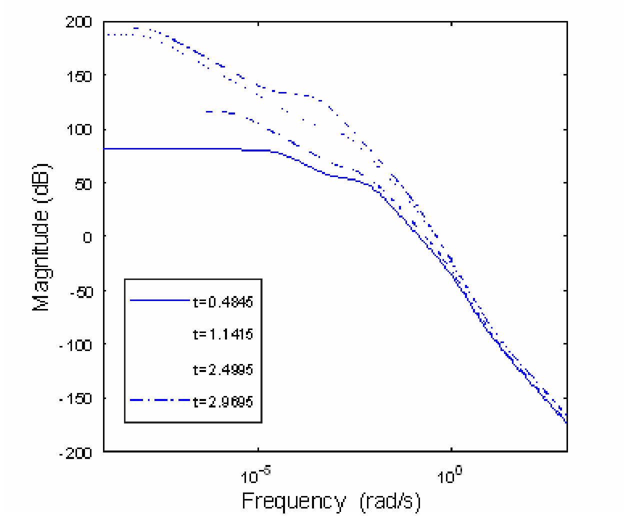

Fig. 10–Bode plot of δ_r to y

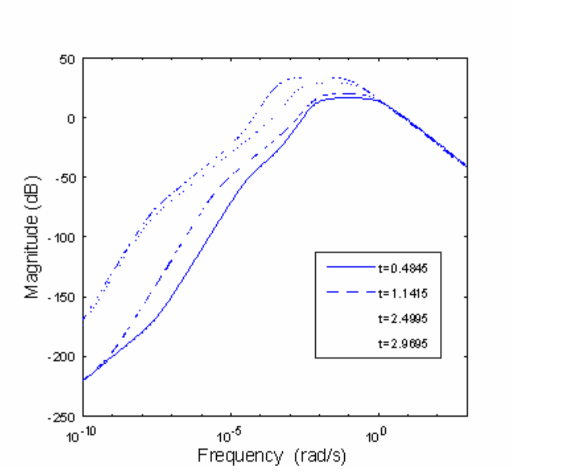

Fig. 11–Bode plot of δ_s to r.

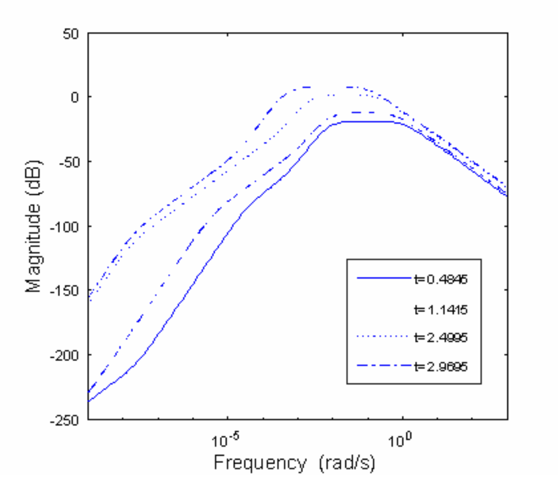

Fig. 12–Bode plot of δ_r to r.

5.3. OUTPUT OF UAV WITH DISTURBANCE

The disturbance is introduced to the UAV in the form of wind perturbation which as an input influences the linear velocity v of UAV. The controller tries to bring the UAV to the centerline as soon as possible in the presence of disturbance. The UAV is first given a disturbance of wind magnitude of 2m/s followed by a disturbance of 6 m/s. Figure 13 shows the effect on y with controller and without controller. The plots illustrate the effectiveness of the controller in that the output follows the reference trajectory. Figure 14 shows the effect on ψ with controller and without controller. Same phenomenon is observed with output r in Fig. 15 as controller is effective in bringing it back to zero (reference). Table 2 shows the maximum error in output y, r and ψ with the wind magnitude of 2 m/s and 6 m/s. Overall it can be seen that the performance of the controller is relatively better at the wind magnitude 2 m/s. As the magnitude of disturbance increases, the controller still tries to track the reference though with reduced efficiency.

Table 2

Max error in output with wind of mag 2m/s and 6m/s

Output	Max error with wind of mag 2m/s	Max error with wind of mag 6m/s
y (m)	0	0
r (deg/s)	0.0145	0.1746
Ψ (deg)	0.0298	0.0843

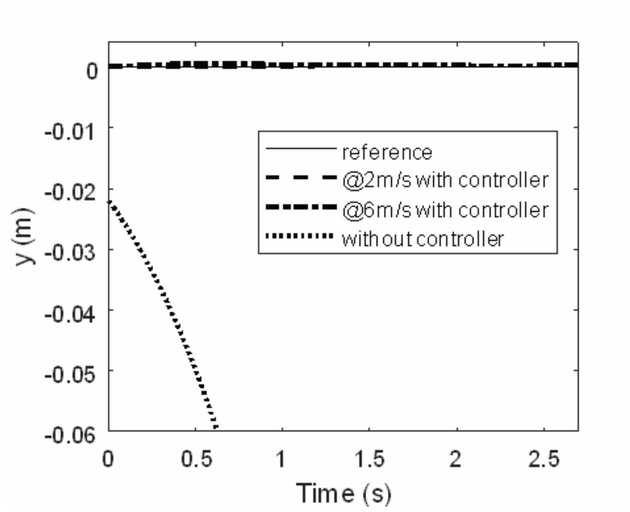

Fig.13–Effect of wind on y.

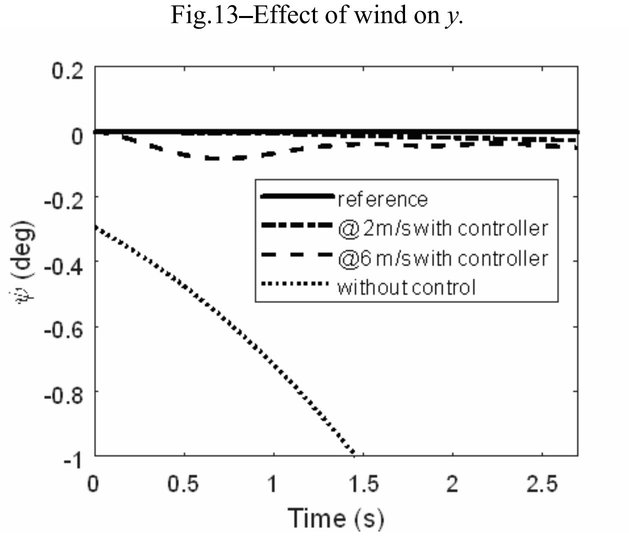

Fig. 14–Effect of wind on ψ.

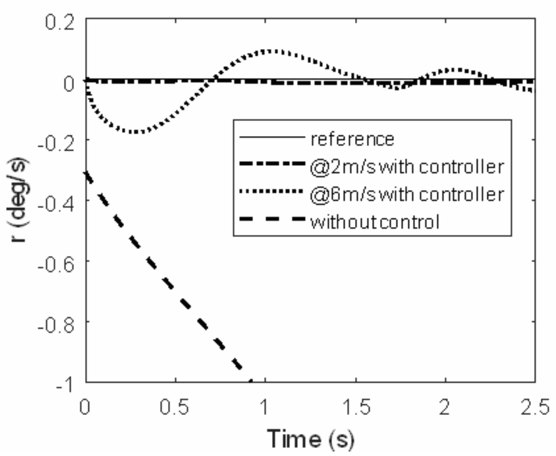

Fig. 15–Effect of wind on r.

5.4. INPUT OF UAV WITH AND WITHOUT DISTURBANCE

The inputs to UAV that are the steering angle δ_s and the rudder δ_r have physical limitations. Saturation has been applied in Simulink to ensure that the UAV inputs do not go out of the physical limit. Without any disturbance both the inputs δ_r and δ_s remain zero. Figures 16 and 17 show plots with wind magnitude 2 m/s and 6 m/s respectively and an angle of 20°. The steering input does not reach saturation in any of the above cases, however in wind magnitude of 6 m/s, the rudder input quickly goes to saturation and stays there for the whole time period of simulation.

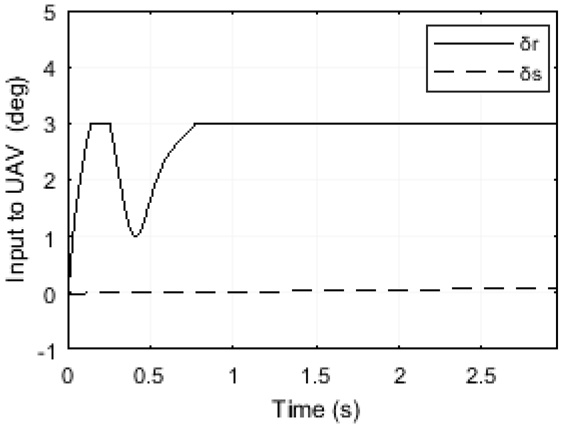

Fig.16–Plot of δ_s and δ_r with a wind of magnitude 2 m/s

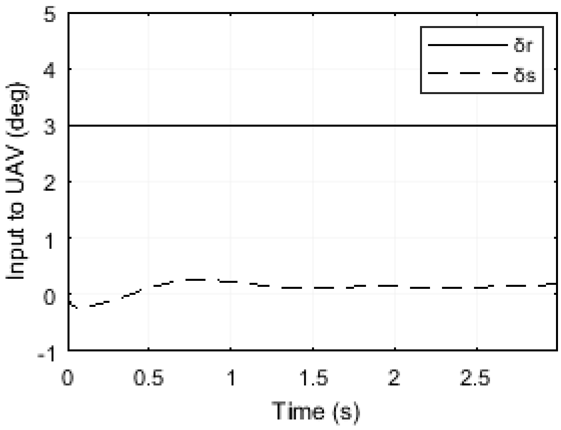

Fig. 17–Plot of δ_s and δ_r with a wind of magnitude 6 m/s

6. CONCLUSION

This work presents a method for analysis and control of a taxi phase of UAV. The main objective is to control the UAV while it is in taxi phase so that it stays on the centerline and even when it is subjected to a disturbance such as wind, the UAV returns back to the centerline. Firstly, to derive the control law for a UAV, a thorough understanding of the dynamics of UAV has to be established. For this purpose, analysis of a given UAV taxi model is performed so as to establish which control technique is most suitable and which input channels are most effective for the control.

After analysis, it has been concluded that since the UAV taxi model is non-linear in nature and has varying dynamics at different time instances, therefore the suitable control strategy is GS-PID.

Simulation results demonstrated that the UAV returns to the centerline in less than 3 seconds. The designed control law successfully tracks the reference trajectory even in the presence of wind of mag 6 m/s. This control strategy can now be implemented on this particular UAV which is being used for defense purpose.

Received on February 17, 2018

REFERENCES

1. J. Iqbal, R. U. Islam, S. Z. Abbas, A. A. Khan, S. A. Ajwad, *Automating industrial tasks through mechatronic systems–A review of robotics in industrial perspective*, Tehnički vjesnik, **23**, pp. 917-924, 2016.
2. O. Khan, M. Pervaiz, E. Ahmad, J. Iqbal, *On the derivation of novel model and sophisticated control of flexible joint manipulator*, Revue Roumaine Des Sciences Techniques-Serie Electrotechnique Et Energetique, **62**, pp. 103-108, 2017.
3. J. Iqbal, M. Ullah, S. G. Khan, B. Khelifa, S. Ćuković, *Nonlinear control systems-A brief overview of historical and recent advances*, Nonlinear Engineering, **6**, pp. 301-312, 2017.
4. B. Yan, C. Wu, *Research on taxi modeling and taking-off control for UAV*, in Computational Intelligence and Design (ISCID), Seventh International Symposium, pp. 108-111, 2014.
5. M. Essuri, K. Alkurmaji, A. Ghmmam, *Developing a dynamic model for unmanned aerial vehicle motion on ground during takeoff phase*, in Applied Mechanics and Materials, 2012, pp. 561-567.
6. H. Song, X. Chen, *Model and auto take-off control law design of unmanned aerial vehicle*, in Advanced Materials Research, pp. 1524-1530, 2012.
7. H. Xiong, F.-s. Jing, J.-q. Yi, G.-l. Fan, IEEE International Conference on Automatic takeoff of unmanned aerial vehicle based on active disturbance rejection control, Robotics and Biomimetics (ROBIO), pp. 2474-2479, 2009.
8. J. Gao, H. Jia, *Control research for a small fixed-wing UAV during ground taxiing*, Journal of Harbin Institute of Technology,**2**, pp. 8-13, 2017.
9. P. Poksawat, L. Wang, A. Mohamed, *Automatic tuning of attitude control system for fixed-wing unmanned aerial vehicles*, IET Control Theory & Applications, **10**, pp. 2233-2242, 2016.
10. P. Poksawat, L. Wang, A. Mohamed, *Gain scheduled attitude control of fixed-wing UAV with automatic controller tuning*, *I*EEE Transactions on Control Systems Technology, 2017.
11. J. R. Hervas, M. Reyhanoglu, H. Tang, and E. Kayacan, "Nonlinear control of fixed-wing UAVs in presence of stochastic winds," *Communications in Nonlinear Science and Numerical Simulation,* vol. 33, pp. 57-69, 2016.
12. T. Stastny, A. Dash, and R. Siegwart, "Nonlinear mpc for fixed-wing uav trajectory tracking: Implementation and flight experiments," in *AIAA Guidance, Navigation, and Control (GNC) Conference*, 2017.
13. S. U. Ali, R. Samar, and M. Z. Shah, "UAV lateral path following: Nonlinear sliding manifold for limited actuation," in *Control Conference (CCC), 36th Chinese*, 2017, pp. 1348-1353.
14. O. Grigore-Mueler, M. A. Barbelian, Artificial intelligence automatic flight control system with gain scheduling, Revue Roumaine Des Sciences Techniques-Serie Electrotechnique Et Energetique, **54**, pp. 105-114, 2009.
15. O. Grigore-Müler, *A neural controller for on board tracking platform*, Revue Roumaine Des Sciences Techniques-Serie Electrotechnique Et Energetique, **54,** pp. 213-222, 2009.